Spectroscopic and Geometric Variations in Perturbed Blue Copper Centers: Electronic Structures of Stellacyanin and Cucumber Basic Protein

Louis B. LaCroix,[†] David W. Randall,[†] Aram M. Nersissian,[‡] Carla W. G. Hoitink,[§] Gerard W. Canters,[§] Joan S. Valentine,[‡] and Edward I. Solomon*,[†]

Contribution from the Department of Chemistry, Stanford University, Stanford, California 94305, Department of Chemistry and Biochemistry, University of California, Los Angeles, California 90095, and Department of Chemistry, Gorlaeus Laboratories, Leiden University, P.O. Box 9502, 2300 RA Leiden, The Netherlands

Received February 23, 1998

Abstract: The electronic structures of the perturbed blue copper proteins stellacyanin (STC) and cucumber basic protein (CBP, also called plantacyanin, PNC) are defined relative to that of the well-understood "classic" site found in plastocyanin (PLC) by combining the results of low-temperature optical absorption, circular dichroism, and magnetic circular dichroism spectra with density functional calculations. Additionally, absorption and magnetic circular dichroism spectra of *Alcaligenes denitrificans* wild-type and M121Q azurin are presented and compared to PLC and STC, respectively. These studies show that the principal electronic structure changes in CBP/PNC, with respect to PLC, are a small shift of the ligand field transitions to higher energy and a rotation of the Cu $d_{x^2-y^2}$ half-filled HOMO which increases the pseudo-σ and decreases the π interactions of the cysteine (Cys) sulfur with Cu $d_{x^2-y^2}$ and, in addition, mixes some methionine (Met) sulfur character into the HOMO. The geometrical distortion responsible for the perturbed electronic structure, relative to PLC, involves a coupled angular movement of the Cys and Met residues toward a more flattened *tetragonal* structure. In contrast to CBP/PNC, STC (which has the axial Met substituted by Gln) has its ligand field transitions shifted to lower energy and undergoes much smaller degrees of HOMO rotation and Cys pseudo-σ/π mixing; no axial glutamine character is displayed in the HOMO. These changes indicate a *tetrahedral* distortion in STC. Therefore, *perturbed spectral features are consistent with both tetragonal and tetrahedral geometric distortions relative to PLC*. These perturbations are discussed in terms of the increased axial ligand strength in these proteins (i.e., short Cu−S(Met) in CBP/PNC and Oϵ(Gln) in STC). This induces an $\sim\epsilon$(u)-like distorting force which either results in a tetragonal distortion of the site (CBP/PNC) or is structurally restrained by the protein (STC and M121Q).

Introduction

Blue (type 1) copper proteins exhibit rapid electron-transfer rates and high redox potentials compared with tetragonal "normal" copper complexes.[1−4] Perhaps the most striking features of such proteins are an intense absorption at ∼600 nm and a small $A_{\|}$ value in the EPR spectra.[5,6] These features reflect novel electronic structures which contribute to reactivity.[6−9]

Classic blue copper proteins, such as plastocyanin and azurin, show intense ∼600 nm bands, a weak absorption envelope at ∼450 nm ($R_\epsilon = \epsilon_{450}/\epsilon_{600} < \sim 0.15$) and display approximately axial ($g_x \approx g_y$) EPR signals. These spectral features derive from the Cu site's distorted C_{3v} tetrahedral ligand set in which two histidine (His) N's with typical Cu−N bonds (∼2.0 Å) and a highly covalent cysteine (Cys) S with an unusually short Cu−S bond (∼2.1 Å) form an approximate trigonal plane which contains the half-occupied Cu $d_{x^2-y^2}$ based HOMO. A weak axial ligand completes the site (usually a long methionine (Met) Cu−S bond at ∼2.8 Å).[10] A strong π S(Cys)-Cu interaction orients the $d_{x^2-y^2}$ orbital so that the Cu−S(Cys) bond bisects the lobes of this orbital and is responsible for the intense S(Cys) p → Cu $3d_{x^2-y^2}$ transition at 600 nm.[8,11]

Type 1 centers which exhibit spectral features[12,13] substantially varied from those of the well-defined classic center are

* Author to whom correspondence should be addressed.
[†] Stanford University.
[‡] University of California, Los Angeles.
[§] Leiden University.

(1) Gray, H. B.; Solomon, E. I. In *Copper Proteins*; Spiro, T. G., Ed.; Wiley: New York, 1981; pp 1−39.
(2) Adman, E. T. In *Topics in Molecular and Structural Biology: Metalloproteins*; Harrison, P., Ed.; MacMillan: New York, 1985; Vol. 1, pp 1−42.
(3) Adman, E. T. In *Advances in Protein Chemistry*; Anfinsen, C. B., Richards, F. M., Edsall, J. T., Eisenberg, D. S., Eds.; Academic Press: San Diego, CA 1991; Vol. 42, pp 145−198.
(4) Sykes, A. G. *Adv. Inorg. Chem.* **1991**, *36*, 377−408.
(5) Penfield, K. W.; Gewirth, A. A.; Solomon, E. I. *J. Am. Chem. Soc.* **1985**, *107*, 4519−4529.
(6) Solomon, E. I.; Baldwin, M. J.; Lowery, M. D. *Chem. Rev.* **1992**, *92*, 521−542.
(7) Solomon, E. I.; Lowery, M. D. *Science* **1993**, *259*, 1575−1581.
(8) Solomon, E. I.; Penfield, K. W.; Gewirth, A. A.; Lowery, M. D.; Shadle, S. S.; Guckert, J. A.; LaCroix, L. B. *Inorg. Chim. Acta* **1996**, *243*, 67−78.
(9) Lowery, M. D.; Guckert, J. A.; Gebhard, M. S.; Solomon, E. I. *J. Am. Chem. Soc.* **1993**, *115*, 3012−3013.
(10) Guss, J. M.; Bartunik, H. D.; Freeman, H. C. *Acta Crystallogr.* **1992**, *B48*, 790−811.
(11) Gewirth, A. A.; Solomon, E. I. *J. Am. Chem. Soc.* **1988**, *110*, 3811−3819.
(12) Lu, Y.; LaCroix, L. B.; Lowery, M. D.; Solomon, E. I.; Bender, C. J.; Peisach, J.; Roe, J. A.; Gralla, E. B.; Valentine, J. S. *J. Am. Chem. Soc.* **1993**, *115*, 5907−5918.

S0002-7863(98)00606-4 CCC: $15.00
Published on Web 09/05/1998

referred to as "perturbed" blue copper centers. Perturbed blue copper sites, such as those in stellacyanin (STC), cucumber basic protein (CBP), *Achromobacter cycloclastes* nitrite reductase (NiR), and pseudoazurin, exhibit rhombic EPR signals (i.e., $\Delta g_\perp = g_x - g_y > 0.01$) and increased 450 nm absorption intensities relative to those in classic blue copper proteins, usually accompanied by a decrease in the blue band intensity ($R_\epsilon > \sim 0.15$). Such perturbed spectral features are observed in cases where the classic blue Cu ligands ($CysHis_2Met$) are retained (i.e., cucumber basic protein, nitrite reductase, etc.) and when they are not (i.e., stellacyanin). The recently available structure[14] of stellacyanin shows that the prototypical axial Sδ(Met) ligand is replaced by an amide oxygen from a glutamine side chain (Oϵ(Gln)).

Our previous study[15] on the perturbed site (i.e., green) in *A. cycloclastes* nitrite reductase ($R_\epsilon = 1.2$[16]) demonstrated this to be tetragonally distorted (toward square planar), in contrast to the tetrahedral distortion proposed for this site on the basis of resonance Raman measurements.[17,18] To understand the electronic and geometric structure origins of the spectral features across the entire range of perturbed sites, blue centers with lesser degrees of perturbation and different axial ligation from nitrite reductase must be examined. Cucumber basic protein (also called plantacyanin, PNC)[19,20] ($R_\epsilon \approx 0.6$, $\Delta g_\perp \approx 0.04$) and *Rhus vernicifera* stellacyanin[21,22] (STC) ($R_\epsilon \approx 0.2$, $\Delta g_\perp \approx 0.05$) both exhibit perturbed spectral features and allow for a comparison of Met and Gln axial ligation. The active site structures of CBP[10] and STC[14] are summarized in Figure 1. Compared with plastocyanin, in cucumber basic protein the Cu−S(Cys) bond has expanded by 0.1 Å and the Cu−S(Met) has contracted by 0.2 Å.[10] The most prominent difference between *Cucumis sativa* (cucumber) stellacyanin and plastocyanin is the replacement of the S(Met) axial ligand with O(Gln) at a distance of ~2.2 Å; however, the Cu−S(Cys) bond also lengthens by 0.1 Å relative to plastocyanin.[14]

In this study, the electronic structure of the active sites in cucumber basic protein and stellacyanin are defined relative to that of the classic blue copper site in plastocyanin in order to describe the differences in bonding associated with the spectral changes and electronic effects on the geometry of the site. The energies and intensities of the excited-state spectral features are obtained from low-temperature absorption (Abs), circular dichroism (CD), and magnetic circular dichroism (MCD) spectroscopies.[23] Density-functional calculations are used to probe further the electronic structure of these perturbed blue Cu proteins. The study presented here also provides an experimental and theoretical description of the electronic structure of a blue copper protein with an axial ligand other than methionine. Combined with previous results,[15] these results allow for spectroscopic trends and their origins to be examined across the range of classic to perturbed proteins (both methionine and non-methionine containing). Finally, spectroscopic correlations between classic wild-type *Alcaligenes denitrificans* azurin ($R_\epsilon \approx 0.1$, $\Delta g_\perp \approx 0.01$) and its perturbed axial mutant Gln M121Q[24] ($R_\epsilon \approx 0.2$, $\Delta g_\perp \approx 0.05$) provide further insight into possible protein contributions to active site electronic and geometric structure of perturbed relative to classic blue copper centers.

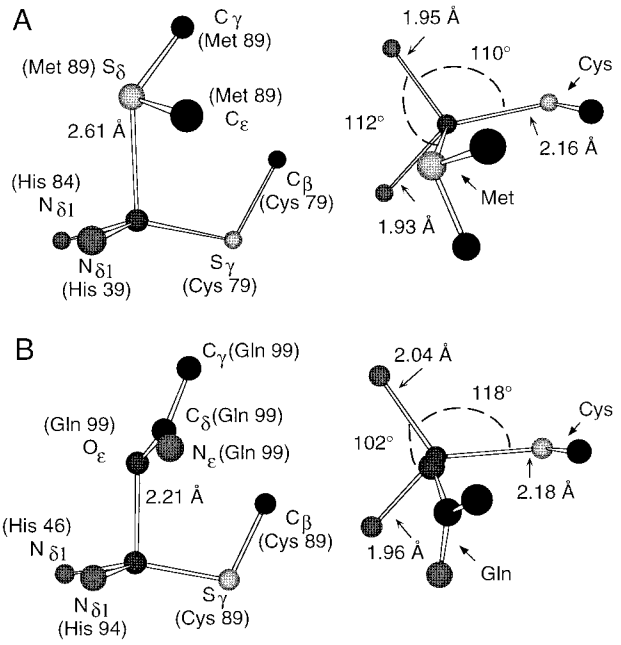

Figure 1. Structure of the oxidized blue copper centers in (A) cucumber basic protein[38] (B) and *Cucumis sativus* stellacyanin[14] viewed with the cysteine−histidine−histidine (Cys−His−His) NNS plane perpendicular (left) and parallel (right) to the plane of the paper. The angular orientation of the Cys, Met, and Gln ligands in relation to the His ligands is most apparent in the parallel view.

Experimental Section

Low-Temperature Optical Spectra. Low-temperature absorption, circular dichroism (CD), and magnetic circular dichroism (MCD) spectra were obtained and fit as described in ref 15. *Rhus vernicifera* stellacyanin,[25] wild type and M121Q forms of *A. denitrificans* azurin,[24] and cucumber basic protein[26] were prepared as described elsewhere. Protein samples (~0.5−1.0 mM) were prepared as glasses in 50% (v/v) D_2O/glycerol−d_3 in either 50 mM phosphate (pD* = 7.6) (cucumber basic protein), 10 mM phosphate (pD* = 6.0) (stellacyanin), or 20 mM phosphate (pD* = 7.0) (wild type and M121Q azurin).

Electronic Structure Calculations. A. Active Site Geometry. In the C_1(met)(his) approximation of the active site in cucumber basic protein used, the oxidized blue copper site is modeled by $Cu[(S(CH_3)_2)(SCH_3)(C_3N_2H_4)_2]^+$. The blue site in stellacyanin was modeled by the C_1(gln)(his) approximation, where acetamide (CH_3CONH_2), occupies the axial position. The crystallographically determined coordinates were used for all atoms except hydrogens, which were added in appropriate geometries to complete the site. Each blue copper center was placed

(13) Han, J.; Loehr, T. M.; Lu, Y.; Valentine, J. S.; Averill, B. A.; Sanders-Loehr, J. *J. Am. Chem. Soc.* **1993**, *115*, 4256−4263.
(14) Hart, P. J.; Nesissian, A. M.; Herrmann, R. G.; Nalbandyan, R. M.; Valentine, J. S.; Eisenberg, D. *Protein Sci.* **1996**, *5*, 2175−2183.
(15) LaCroix, L. B.; Shadle, S. E.; Wang, Y.; Averill, B. A.; Hedman, B.; Hodgson, K. O.; Solomon, E. I. *J. Am. Chem. Soc.* **1996**, *118*, 7755−7769.
(16) Liu, M.-Y.; Liu, M.-C.; Payne, W. J.; LeGall, J. *J. Bacteriol.* **1986**, *166*, 604−608.
(17) Andrew, C. R.; Yeom, H.; Valentine, J. S.; Karlsson, B. G.; Bonander, N.; van Pouderoyen, G.; Canters, G. W.; Loehr, T. M.; Sanders-Loehr, J. *J. Am. Chem. Soc.* **1994**, *116*, 11489−11498.
(18) Andrew, C. R.; Sanders-Loehr, J. *Acc. Chem. Res.* **1996**, *29*, 365−372.
(19) Aikazyan, V. T.; Nalbandyan, R. M. *FEBS Lett.* **1975**, *55*, 272−274.
(20) Sakurai, T.; Okamoto, H.; Kawahara, K.; Nakahara, A. *FEBS Lett.* **1982**, *147*, 220−224.
(21) Peisach, J.; Levine, W. G.; Blumberg, W. E. *J. Biol. Chem.* **1967**, *242*, 2847−2858.
(22) Malmström, B. G.; Reinhammar, B.; Vänngård, T. *Biochim. Biophys. Acta* **1970**, *205*, 48−57.
(23) Solomon, E. I.; Hanson, M. A. In *Inorganic Electronic Spectroscopy*; Solomon, E. I., Lever, A. P. B., Eds.; Wiley & Sons: New York, 1998, in press.
(24) Romero, A.; Hoitink, C. W. G.; Nar, H.; Huber, R.; Messerschmidt, A.; Canters, G. W. *J. Mol. Biol.* **1993**, *229*, 1007−1021.
(25) Reinhammar, B. *Biochim. Biophys. Acta* **1970**, *205*, 35−47.
(26) Nersissian, A. M.; Nalbandyan, R. M. *Biochim. Biophys. Acta* **1988**, *957*, 446.

in a coordinate system chosen to give a Cu $d_{x^2-y^2}$ ground state wave function, which is experimentally observed from the *g* values in the EPR spectrum of each site ($g_{\|} > g_{\perp} > 2.0$):[19−22] the Cu−S(Cys) bond is 45° from the *x* and *y* axes, while the bond closest to *z* is Cu−S(Met) or O(Gln). This axis system diagonalizes the *g*-tensor for plastocyanin.[11] The Cartesian coordinates for calculations performed in this study on the cucumber basic protein and stellacyanin active sites are provided as Supporting Information.

B. SCF-Xα-SW Calculations. The 1982 QCPE release of the SCF-Xα-SW package[27−30] was used to evaluate the electronic structure of cucumber basic protein and stellacyain as described in ref 15. Atomic sphere radii adjusted to reproduce the experimental *g* values in plastocyanin were employed for all calculations.[11] The oxygen sphere radius in the stellacyanin calculations was set to 1.70 Bohr on the basis of the Norman criteria.[31] The parameters used for the SCF-Xα-SW calculations are listed as Supporting Information.

C. LCAO Density Functional Calculations. Spin restricted calculations were performed as described previously[15] using version 1.1.3 of the Amsterdam Density Functional (ADF) programs of Baerends and co-workers.[32] Basis functions, core expansions functions, core coefficients, and fit functions for all atoms were used as provided from database IV, which includes Slater-type orbital triple-ζ basis sets for all atoms and a single-ζ polarization function for all atoms except Cu.

Results and Analysis

Electronic Structure of Cucumber Basic Protein. A. Optical Spectroscopic Parameters. Low-temperature absorption, MCD, and CD spectra between 5000 and 30000 cm^{-1} for cucumber basic protein are presented in Figure 2. Simultaneous Gaussian resolution of these spectra requires eight bands to adequately fit the spectra and are included in top panel of Figure 2. Three bands (1−3) with approximately equal intensity are required to fit the ∼450 nm absorption transition envelope. A single transition (4) accounts for the intensity under the ∼600 nm band. Two transitions (5−6) and a portion of a third (7) contribute to the ∼750 nm band. The positions and relative intensities of the individual bands are easier to envision by inspection of the MCD and CD spectra (Figure 2). While the position and intensity of band 2 cannot be determined from the MCD spectrum, the presence of this band is required by the intense negative CD feature found at ∼22500 cm^{-1} for which bands 1 and 3 cannot account. The lowest energy band (8) is required by the MCD spectrum.

The transition energies and ϵ values, at the absorption band maxima, are summarized in Table 1. Experimental oscillator strengths, f_{exp}, listed in Table 1 have been calculated through the fitted absorption maxima and full widths at half-maxima according to the approximation

$$f_{exp} \approx 4.61 \times 10^{-9}\, \epsilon_{max}\, \bar{\nu}_{1/2} \qquad (1)$$

where the absorption maximum, ϵ_{max}, is expressed in M^{-1} cm^{-1} and $\bar{\nu}_{1/2}$, the full width at half-maximum of the absorption band, is in cm^{-1}. All features in the MCD spectrum of cucumber basic protein consist of *C*-term intensity and have magnetization−saturation curves that can be fit to an isotropic $g \approx 2.1$,

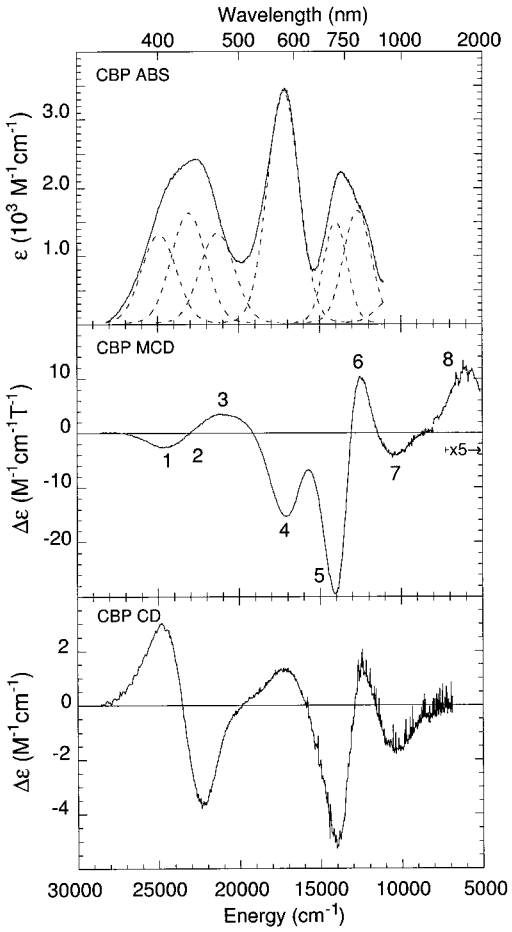

Figure 2. Electronic absorption (top), magnetic circular dichroism (middle), and circular dichroism (bottom) spectra of cucumber basic protein. Abs, MCD, and CD spectra were obtained at 4.2 K on 0.05 M phosphate (pD* 7.0)/glycerol-d_3 glasses (50:50 v/v). Gaussian resolution of bands in the absorption spectra is based on a simultaneous linear least-squares fit of the Abs, MCD, and CD data. The numbering scheme is chosen to be consistent with the assignments of bands in plastocyanin (see Table 1 for assignments). The position and intensity of band 2 cannot be resolved in the MCD spectrum; however, its presence is required by the CD data.

which is consistent with the Cu(II) ground-state EPR spectrum.[19,20] To differentiate ligand field from charge-transfer transitions C_0/D_0 ratios are particularly valuable since this ratio is sensitive the amount of metal character in the particular excited state (vide infra). For complexes exhibiting only *C*-term MCD intensity, C_0/D_0 ratios can be determined from the $\Delta\epsilon$ and ϵ values obtained from the Gaussian fit of the MCD spectrum (Table 1) taken within the linear $1/T$ region and the absorption spectrum,[33] respectively *via*

$$\frac{C_0}{D_0} = \frac{kT}{\mu_B B}\left(\frac{\Delta\epsilon}{\epsilon}\right)_{max} \qquad (2)$$

where T is the temperature, B is the external magnetic field strength, k is Boltzmann's constant, μ_B is the Bohr magneton, ϵ is the absorption maximum in M^{-1} cm^{-1}, and $\Delta\epsilon$ is MCD intensity maximum measured in M^{-1} cm^{-1} ($k/\mu_B \approx 1.489$ T K^{-1}).

B. SCF-Xα-SW Calculations. The SCF-Xα-SW calculated ground-state energies and one-electron wave functions for the

(27) Johnson, K. H.; Norman, J. G., Jr.; Connolly, J. W. D. In *Computational Methods for Large Molecules and Localized States in Solids*; Herman, F., McLean, A. D., Nesbet, R. K., Eds.; Plenum: New York, 1973; pp 161−201.
(28) Rosch, N. In *Electrons in Finite and Infinite Structures*; Phariseu, P., Scheire, L., Eds.; Wiley: New York, 1977.
(29) Slater, J. C. *The Calculation of Molecular Orbitals*; John Wiley & Sons: New York, 1979.
(30) Connolly, J. W. D. In *Modern Theoretical Chemistry*; Segal, G. A., Ed.; Plenum: New York, 1977; Vol. 7, pp 105−132.
(31) Norman, J. G., Jr. *Mol. Phys.* **1976**, *31*, 1191−1198.
(32) te Velde, G.; Baerends, E. J. *J. Comput. Phys.* **1992**, *99*, 84−98.
(33) Piepho, S. B.; Schatz, P. N. *Group Theory in Spectroscopy With Applications to Magnetic Circular Dichroism*; John Wiley & Sons: New York, 1983.

Table 1. Experimental Spectroscopic Parameters for Cucumber Basic Protein (with Plastocyanin Parameters[15] for Comparison)

band	assignments in PLC[11]	energy (cm^{-1})			ϵ (M^{-1} cm^{-1})		f_{exp} oscillator strength		$\Delta\epsilon$ (M^{-1} cm^{-1} T^{-1}) at 4.2 K		C_0/D_0	
		CBP	PLC	diff[a]	CBP	PLC	CBP	PLC	CBP	PLC	CBP	PLC
8	d_{z^2}	5800	5000	800					+2.6	(+)[c]	(+)[c]	(+)[c]
7	d_{xy}	10800	10800	0	300	250	0.0030	0.0031	−4.5	−8.5	−0.093	−0.213
6	d_{xz+yz}	12900	12800	100	1640	1425	0.0151	0.0114	+15.3	+20.9	+0.058	+0.092
5	d_{xz-yz}	14100	13950	150	1480	500	0.0121	0.0043	−35.0	−41.4	−0.148	−0.518
4	Cys π	17100	16700	400	3410	5160	0.0381	0.0496	−15.2	−10.2	−0.028	−0.012
3	pseudo-σ	21000	18700	2300	1320	600	0.0150	0.0048	+3.8	+1.2	+0.018	+0.013
2	His π_1	22500	21390	1110	1610	288	0.0185	0.0035	*b*	−0.5	*b*	−0.011
1	Met[d]	24750	23440	1310	1290	250	0.0148	0.0030	−2.7	−0.5	−0.013	−0.013

[a] Difference in transition energies (defined as cucumber basic protein minus plastocyanin energy). [b] The position and intensity of band 2 cannot be determined from the MCD data; however, its presence is required by the CD spectrum. [c] Only signs can be determined from the data for these parameters;[35] however, the C_0/D_0 ratios should be greater than 0.1 based on the relative magnitude of MCD to upper ϵ limit in absorption. [d] This likely involves the Met b_1 orbital. See Ref 15 for details.

Table 2. Results of SCF-Xα-SW Calculations for the Highest Occupied Valence Orbitals of the C_1(met)(his) Site in CBP

level	orbital label	energy (eV)	%Cu				% Cu d orbital breakdown[c]					%Cys		%Met		%His	
			Cu[a]	*s*[b]	*p*[b]	*d*[b]	d_{z^2}	d_{xz}	d_{yz}	$d_{x^2-y^2}$	d_{xy}	S	Cys[d]	S	Met[d]	N[e]	His[d]
48 a	Cu $d_{x^2-y^2}$	-2.75	58	*1*	*2*	*52*	1.4	0.4	0.4	49.5	0.2	29	2	2	0	6	2
47 a	Cu d_{xy}	-3.24	58	*2*	*7*	*46*	0.0	16.8	8.7	0.1	20.4	26	2	8	0	2	2
46 a	Cu d_{z^2}	-3.73	78	*0*	*4*	*73*	29.4	17.5	0.4	11.1	14.6	2	1	10	2	3	2
45 a	Cu d_{xz-yz} [f]	-4.00	79	*0*	*2*	*75*	4.1	4.7	65.0	0.9	0.3	5	1	0	0	0	9
44 a	Cu d_{xz+yz} [f]	-4.12	82	*0*	*1*	*78*	6.4	44.2	5.2	11.4	10.8	8	1	1	0	3	5
43 a	Cys π	-4.46	52	*0*	*4*	*45*	3.7	16.2	3.5	12.4	9.2	32	4	0	0	5	7
42 a	His π_1	-4.68	14	*0*	*0*	*13*	3.8	1.9	0.3	0.3	6.8	1	0	2	0	8	75
41 a	His π_1	-4.87	13	*0*	*1*	*10*	2.6	0.7	3.5	0.8	2.4	2	0	14	2	8	50
40 a	Met b_1	-5.03	30	*3*	*1*	*25*	2.1	14.5	1.4	1.9	5.1	0	0	45	8	2	15
39 a	Cys pseudo-σ	-5.47	40	*2*	*5*	*31*	5.9	0.1	6.0	2.8	17.2	49	8	0	0	1	1
38 a	His π_2	-6.50	8	*0*	*0*	*6*	0.1	3.8	0.5	0.0	1.6	0	0	6	3	44	36
37 a	Met a_1	-7.02	8	*0*	*2*	*4*	1.2	1.6	0.4	0.4	0.5	5	3	47	29	5	3
36 a	Cys σ	-7.26	19	*0*	*3*	*11*	0.3	0.4	7.2	1.7	0.7	41	26	4	2	4	2
35 a	His π_2	-7.48	7	*0*	*2*	*3*	0.8	0.1	0.1	0.0	2.0	6	4	0	0	44	37

[a] Total charge on the copper ion. [b] *l* quantum breakdown for the copper ion. [c] Specific d orbital contributions to the total Cu d charge. [d] Total charge for all atoms of the ligand except the S or N coordinated to Cu. [e] Total charge for the coordinating N atoms. [f] These labels are only strictly valid for C_s symmetry; in the lower symmetry used here, variable amounts of mixing between these orbitals can occur.

highest occupied valence orbitals obtained for the C_1(met)(his) approximation of the cucumber basic protein active site are presented in Table 2. Reference 15 describes SCF-Xα-SW calculations on the C_1(met)(his) sites in plastocyanin and nitrite reductase.

The properties of the redox active, half-occupied HOMO directly affect the electron-transfer reactivity of the site. The origins of many of the distinctive characteristics of blue sites as well as differences between classic and perturbed blue sites can be observed in the properties of the HOMO (vide infra). Similar to plastocyanin, the cucumber basic protein $d_{x^2-y^2}$ based HOMO (level 48 a, Table 2) is highly covalent (52% Cu d character, the same value calculated for PLC[15]), with the predominant Cu−ligand interaction involving 29% S(Cys) and smaller contributions from the ligating S(Met) (2%) and N(His) (6% total) atoms. Contour diagrams for the cucumber basic protein HOMO, plotted perpendicular and parallel to the S(Met)−Cu−S(Cys) plane are shown in Figure 3. These plots reveal the S(Cys)−Cu and S(Met)−Cu interactions. A predominantly π S(Cys)-Cu interaction is clearly evident in the contour plot of the cucumber basic protein HOMO shown in Figure 3A. Several significant Cu−ligand interactions not present in plastocyanin[11] are apparent in the ground-state wave function of cucumber basic protein. Increased pseudo-σ S(Cys)−Cu and S(Met) antibonding interactions in the HOMO can be seen in Figure 3B. Finally, the 1.4% d_{z^2} character that is mixed into the HOMO (Table 2) has been shown by Gewirth et al.[34] to be sufficient to generate the rhombic splitting of the EPR spectrum.

C. Ligand Field Transitions and Site Geometry. The low symmetry of the blue Cu site removes all orbital degeneracy. In such a situation,[11] the two orthogonal dipole moments required for MCD *C*-term intensity[33] can only be acquired through out of state spin−orbit coupling (SOC). Therefore, the MCD intensities (i.e., C_0/D_0 ratios) will depend on the magnitude of SOC occurring at the centers involved in the transitions. Since the SOC parameter for Cu is greater than that for S or N (ξ_{3d}(Cu) ≈ 828 cm^{-1} > ξ_{3p}(S) ≈ 382 cm^{-1} > ξ_{2p}(N) ≈ 70 cm^{-1}), the Cu-based d → d transitions will exhibit greater C_0/D_0 ratios than the ligand-based charge-transfer transitions.[11]

The four CD and MCD spectral features and signs in the low-energy, ligand field region (bands 5−8) for cucumber basic protein (Figure 2) are qualitatively similar to plastocyanin,[11] exhibiting similar signs and $|C_0/D_0|$ ratios of ∼0.1 (Table 1).[35] Thus, the specific assignments for bands 5−8 can be made to parallel those in plastocyanin (Table 1). The energies of d → d transitions are very sensitive to the ligand field at the copper site: The d → d transitions in cucumber basic protein are observed to be ∼100 cm^{-1} higher energy than their counterparts in plastocyanin. This indicates that the cucumber basic protein type 1 center experiences a slightly greater ligand field strength than that of plastocyanin.[11] Such an increased ligand field would result from a small tetragonal geometric distortion from pseudo-

(34) Gewirth, A. A.; Cohen, S. L.; Schugar, H. J.; Solomon, E. I. *Inorg. Chem.* **1987**, *26*, 1133−1146.

(35) While C_0/D_0 for band 8 cannot be determined from the data, estimates for the lower limit of $\Delta\epsilon$ (>1.0 M^{-1} cm^{-1} T^{-1}) and the upper limit for ϵ (<50 M^{-1} cm^{-1}) indicate that the lower limit of $|C_0/D_0|$ for this band is greater than 0.1.

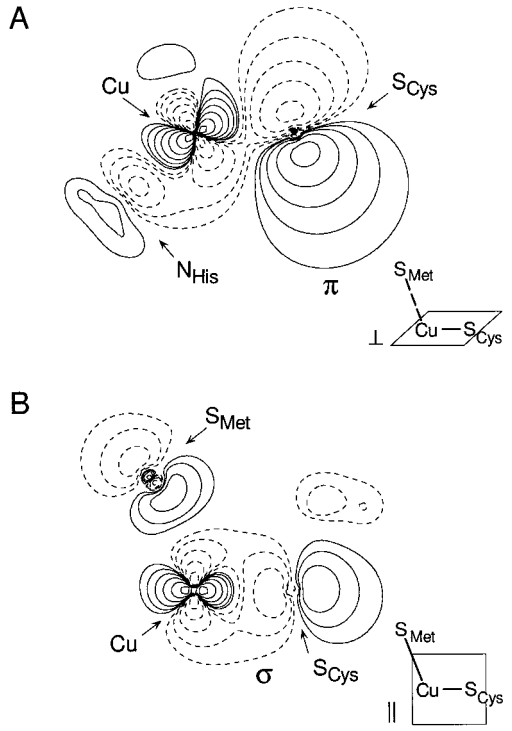

Figure 3. Contours of the highest energy, half-occupied orbital (level 48 a in Table 2) for cucumber basic protein plotted (A) perpendicular and (B) parallel to the S(Cys)−Cu−S(Met) plane. Contour lines are drawn at ±0.64, ±0.32, ±0.16, ±0.08, ±0.04, ±0.02, and ±0.01 (e/Bohr^3)$^{1/2}$.

tetrahedral toward square planar. The EPR spectrum of cucumber basic protein also reflects the increased ligand field by a decrease in g_z relative to plastocyanin (2.207 in CBP[19,20] vs 2.226 in PLC[36]).

In addition to the changes in transition energies, the intensities of the ligand field absorption bands also change. Such changes can reflect differences in bonding, since d → d transitions acquire their intensity from interactions with the higher-energy allowed charge-transfer transitions. Band 5 in the cucumber basic protein absorption spectrum gains considerable intensity while band 6 remains as intense as its counterpart in plastocyanin (Table 1). As in plastocyanin,[11] the high intensity of the Cu $3d_{xz+yz}$ → Cu $3d_{x^2-y^2}$ transition (band 6) is attributed to its having the correct symmetry to gain intensity from the highly allowed blue S(Cys) π → Cu $3d_{x^2-y^2}$ transition through configuration interaction between the orbitals involved in this transition. Analogously, Cu $3d_{xz-yz}$ → Cu $3d_{x^2-y^2}$ (band 5) can gain intensity through mixing with the S(Cys) pseudo-σ → Cu $3d_{x^2-y^2}$ transition (band 3). Therefore, the intensity difference in band 5 absorption in cucumber basic protein relative to plastocyanin support the change in the amount of Cys π and pseudo-σ character mixed into the HOMO described above.

The intensity pattern observed for bands 5 and 6 in cucumber basic protein supports the SCF-Xα-SW calculations in Table 2. The degree to which the individual ligand field transitions borrow intensity from a given charge-transfer transition will be reflected in the amount of the specific d orbital involved in the transition (to the $d_{x^2-y^2}$ HOMO) mixed into the ligand-based orbital. Thus, d_{xz} character in ligand orbitals involved in intense charge-transfer transitions will result in an increase in band 6 intensity, and the presence of d_{yz} character will correspond with band 5 intensity. The Cys π orbital (level 43 a) contains 16.2% d_{xz} character and the Cys pseudo-σ orbital (level 39 a) contains 6.0% d_{yz}. Therefore, it is reasonable for both band 5 and 6 to have sizable intensity, as is observed experimentally. However, the increase in band 5 intensity in cucumber basic protein relative to plastocyanin without a corresponding decrease in band 6 indicates that the intensity redistribution in the ligand field region cannot be only due to Cys π/pseudo-σ mixing. Intensity borrowing from the multiple low-energy, intense charge-transfer bands under the ∼450 nm absorption envelope in Figure 2 is also possible. The significant amount of d_{xz} character (14.5%) found in the Met b_1 orbital (level 40 a, Table 2) indicates that this level is a likely candidate for additional intensity mixing into band 6.

D. Charge-Transfer Transitions and Bonding. The cucumber basic protein absorption spectrum (Figure 2, top) exhibits an intense absorption envelope centered about 450 nm containing sizable contributions from three transitions. Four bands (1−4) with smaller C_0/D_0 ratios (∼0.01, Table 1) can be identified to higher energy than the ligand field transitions (Figure 2). As above, these transitions are charge-transfer transitions; specific assignments can be made through correlation of band energy and CD and MCD features with plastocyanin.[11] Band 4 occurs at similar energy and exhibits the same negative CD and MCD signs as the blue band (band 4 at 598 nm) in plastocyanin.[11] Accordingly, this band is assigned as the S(Cys) π → Cu $3d_{x^2-y^2}$ charge-transfer transition. As in plastocyanin,[11] the single positive charge-transfer feature (band 3) in the MCD of cucumber basic protein is assigned as the S(Cys) pseudo-σ → Cu $3d_{x^2-y^2}$ transition. Band 3 in cucumber basic protein has shifted to higher energy relative to plastocyanin by 2300 cm^{-1} such that it is contained within the ∼450 nm absorption envelope rather than the ∼600 nm envelope.[37]

The absorption intensities in bands 3 and 4 are distributed differently in cucumber basic protein than in plastocyanin. The S(Cys) π → Cu $3d_{x^2-y^2}$ transition (band 4) in cucumber basic protein is reduced in intensity to 3410 M^{-1} cm^{-1} from 5160 M^{-1} cm^{-1} in plastocyanin (Table 1). This decrease in intensity is accompanied by an increase in the pseudo-σ → Cu $3d_{x^2-y^2}$ transition (1320 M^{-1} cm^{-1} vs 600 M^{-1} cm^{-1} in plastocyanin). Since the intensity of these charge-transfer transitions is proportional to the overlap of the cysteine S p and Cu $d_{x^2-y^2}$ orbitals, the increase in intensity for band 3 and the loss of intensity for band 4 relative to plastocyanin indicate a decrease in π and increase in pseudo-σ S(Cys)−Cu overlap in the cucumber basic protein HOMO.

The mixing of π/pseudo-σ character in the HOMO indicated by the experimental data is supported by the results of the SCF-Xα-SW calculations. As can be seen in the contour plot of the cucumber basic protein HOMO (level 48 a, Table 2) (Figure 3), $d_{x^2-y^2}$ is rotated by ∼10° about the molecular *z*-axis (i.e., ∼Cu−S(Met) bond) such that π overlap decreases and pseudo-σ overlap increases in contrast to the purely π interaction in plastocyanin.[11] The increase in pseudo-σ interaction is indicated by the electron density found along the Cu−S(Cys) bond (Figure 3B). This rotation of Cu $d_{x^2-y^2}$ provides a mechanism for the changes in charge-transfer transition intensity observed experimentally, as the charge-transfer transition intensities depend on

(36) Penfield, K. W.; Gay, R. R.; Himmelwright, R. S.; Eickman, N. C.; Norris, V. A.; Freeman, H. C.; Solomon, E. I. *J. Am. Chem. Soc.* **1981**, *103*, 4382−4388.

(37) Conflicting evidence, primarily involving single-crystal polarized absorption and resonance Raman studies, exists regarding whether the S(Cys) pseudo-σ → Cu $3d_{x^2-y^2}$ transition should be attributed to band 2 or 3 in plastocyanin (no conflict exists in the assignments in nitrite reductase). However, bands 2 and 3 are both found under the ∼450 nm absorption band, are of similar intensity, and are significantly more intense than their counterparts in plastocyanin.

the specific ligand orbitals involved in bonding with the HOMO as well as the total ligand character. The degree to which the specific ligand orbitals mix with the HOMO is reflected in the amount of Cu $d_{x^2-y^2}$ character present in the ligand-derived bonding orbitals (Table 2). Relative to plastocyanin,[15] the Cys π/pseudo-σ mixing in cucumber basic protein is characterized by an increase in $d_{x^2-y^2}$ character in the Cys pseudo-σ (level 39a, 2.8% in CBP vs 0.0% in PLC[15]) and a decrease in the Cys π (level 43a, 12.4% in CBP vs 23.9% in PLC[15]) bonding levels. The perturbed type 1 site in nitrite reductase also exhibits Cys π/pseudo-σ mixing in the HOMO, but the degree to which this occurs is larger in the nitrite reductase site where the $d_{x^2-y^2}$ character in Cys π falls to 8.8% while that in pseudo-σ increases to 4.5%, consistent with its experimentally observed higher intensity of the ~450 nm band (band 3 in nitrite reductase) relative to the ~600 nm band (band 4).[15]

The charge-transfer transition intensities in the absorption spectrum also allow for comparison of the total strength of the ligand−metal interaction between sites. The total oscillator strength for the cysteine-based charge-transfer transitions is smaller in cucumber basic protein (0.0531) than in plastocyanin (0.0544) which indicates that, in addition to a shift in the π/σ overlap, the total S(Cys) contribution to the HOMO is less in cucumber basic protein. This finding is consistent with the reduced S(Cys) covalency in the calculated HOMO in Table 2 (level 48 a) (29% in CBP vs 35% in PLC[15]), a lengthening of the Cu−S(Cys) bond by ~0.1 Å,[38] and a decrease of ~30 cm^{-1} in the primary Cu−S(Cys) stretching frequency.[39]

The two transitions (bands 1 and 2 in Figure 2) that are found to be of higher energy than the cysteine-based charge-transfer transitions in cucumber basic protein exhibit considerable absorption intensity increases compared with their counterparts in plastocyanin. In plastocyanin this spectral region exhibits two weak bands assigned as His $\pi_1 \rightarrow$ Cu $3d_{x^2-y^2}$ and Met $\rightarrow$ Cu $3d_{x^2-y^2}$ charge-transfer transitions.[11] In the MCD both are weak and negative, but in the CD His $\pi_1 \rightarrow$ Cu $3d_{x^2-y^2}$ (band 2) is negative while Met $\rightarrow$ Cu $3d_{x^2-y^2}$ (band 1) is positive. Since band 1 in cucumber basic protein has a negative MCD and a positive CD sign, it is assigned as a Met $\rightarrow$ Cu $3d_{x^2-y^2}$ transition, while band 2 has a negative CD sign and is assigned to the His-based transition.

The absorption intensity increase associated with band 1 in cucumber basic protein reflects the fact that S(Met) character is present in the cucumber basic protein HOMO. This finding is supported by the SCF-Xα-SW calculated HOMO wave function, which includes ~2−3% S(Met) character (level 48 a, Table 2) compared to 0% in plastocyanin.[11,15] The reorientation of $d_{x^2-y^2}$ allows for an increased interaction between this orbital and S(Met), as demonstrated in Figure 3B where appreciable electron density is found along the Cu−S(Met) bond. Examination of the Met valence orbitals (Table 2) indicates that the Met b_1 orbital (level 40 a) contains the most $d_{x^2-y^2}$ character (1.9%). The perturbed nitrite reductase HOMO also contains an analogous contribution from the axial methionine (~ 6%).[15] The magnitude of this interaction is greater in nitrite reductase, consistent with the higher intensity of band 1.

In summary, relative to plastocyanin the changes in electronic and geometric structure in cucumber basic protein are similar to the changes which occur in the perturbed type site in nitrite reductase,[15] but are smaller in magnitude. Thus, the perturbed spectral features in the two proteins share common origins: a distortion toward a *tetragonal* geometry that causes a rotation of $d_{x^2-y^2}$ such that a there is significant Cu−S(Cys) pseudo-σ and nonzero Cu−S(Met) overlap in the HOMO in addition to a weakened Cu−S(Cys) bond.

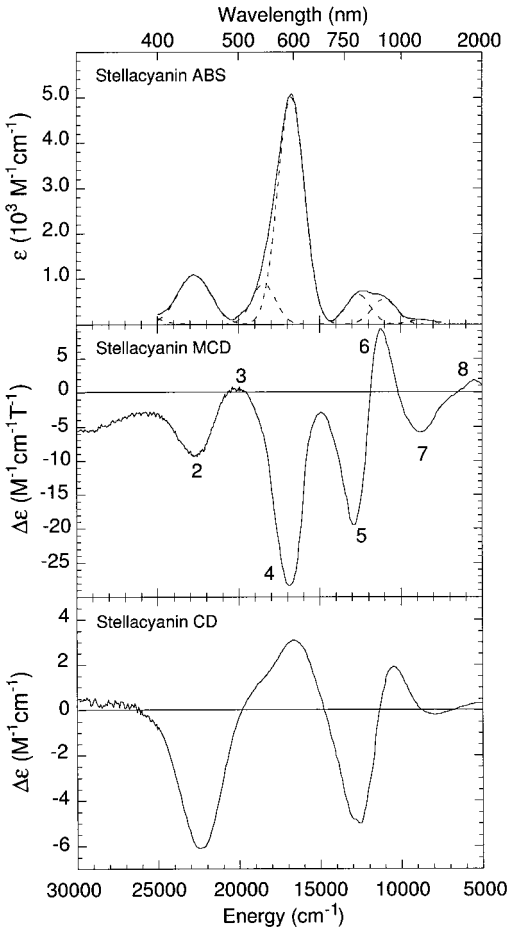

Figure 4. Electronic absorption (top), magnetic circular dichroism (middle), and circular dichroism (bottom) spectra of stellacyanin. Absorption data (adapted from ref 40) were recorded on a thin film at 25 K. MCD and CD spectra were obtained from ref 51 and 41 respectively, except in the regions >19 000 cm^{-1} (MCD) or >25 000 cm^{-1} (CD) which were recorded at 4.2 K in 0.01 M phosphate (pD* 6.0)/glycerol-d_3 glasses (50:50 v/v). Gaussian resolution of bands in the absorption spectra is based on a simultaneous linear least-squares fit of the Abs, MCD, and CD data. The numbering scheme is chosen to be consistent with the assignments of bands in plastocyanin (see Table 3 for assignments). A counterpart for band 1 is not observed.

Electronic Structure of Stellacyanin. A. Optical Spectroscopic Parameters. Low-temperature absorption,[40,41] MCD, and CD spectra between 5000 and 30000 cm^{-1} for stellacyanin are presented in Figure 4. The Gaussian resolution of the absorption spectrum, obtained from a simultaneous fit of the absorption, MCD, and CD spectra is included in the top panel of Figure 4. The transition energies, oscillator strengths, ϵ, $\Delta\epsilon$, and C_0/D_0 values have been determined as presented above (Table 3). All features in the MCD spectrum of stellacyanin exhibit magnetization−saturation behavior consistent with a paramagnetic Cu(II) ground state, and at the low temperatures employed here they consist entirely of *C*-term intensity (as determined from their linear $1/T$ dependence).

In contrast to both classic and perturbed proteins containing an axial S(Met) ligand, only seven bands are required to fit the

(38) Guss, J. M.; Merritt, E. A.; Phizackerley, R. P.; Freeman, H. C. *J. Mol. Biol.* **1996**, *259*, 686−705.
(39) Sakurai, T.; Sawada, S.; Nakahara, A. *Inorg. Chim. Acta* **1986**, *123*, L21 − L22.
(40) Solomon, E. I.; Hare, J. W.; Dooley, D. M.; Dawson, J. H.; Stephens, P. J.; Gray, H. B. *J. Am. Chem. Soc.* **1980**, *102*, 168−178.
(41) Gewirth, A. A., Ph.D. Dissertation, 1987, Stanford University.

Table 3. Experimental Spectroscopic Parameters for Stellacyanin (with Plastocyanin Parameters[15] Included for Comparison)

band	assignments in PLC[11]	energy (cm^{-1})			ϵ (M^{-1} cm^{-1})		f_{exp} oscillator strength		$\Delta\epsilon$ (M^{-1} cm^{-1} T^{-1}) at 4.2 K		C_0/D_0	
		Stc	PLC	diff[a]	Stc	PLC	Stc	PLC	Stc	PLC	Stc	PLC
8	d_{z^2}	5500	5000	500					+1.8	(+)[c]	(+)[c]	(+)[c]
7	d_{xy}	8750	10800	−2050	100	250	0.0009	0.0031	−5.7	−8.5	−0.356	−0.213
6	d_{xz+yz}	11200	12800	−1600	580	1425	0.0048	0.0114	11.6	+20.9	0.105	+0.092
5	d_{xz-yz}	12800	13950	−1150	690	500	0.0056	0.0043	−19.1	−41.4	−0.173	−0.518
4	Cys π	16800	16700	100	4970	5160	0.0439	0.0496	−28.6	−10.2	−0.036	−0.012
3	pseudo-σ	18600	18700	−100	890	600	0.0074	0.0048	+1.8	+1.2	0.013	+0.013
2	His π_1	22750	21390	1350	1090	288	0.0120	0.0035	−9.4	−0.5	−0.054	−0.011
1	Met[d]	*b*	23440		*b*	250	*b*	0.0030	*b*	−0.5		−0.013

[a] Difference in transition energies (defined as stellacyanin minus plastocyanin energy). [b] This band is not observed in the stellacyanin data. [c] Only signs can be determined from the data for these parameters;[35] however, the C_0/D_0 ratios should be greater than 0.1 based on the relative magnitude of MCD to upper ϵ limit in absorption. [d] This likely involves the Met b_1 orbital. See Ref 15 for details.

Table 4. Results of SCF-Xα-SW Calculations for the Highest Occupied Valence Orbitals of the C_1(gln)(his) Site in Stellacyanin

level	orbital label	energy (eV)	%Cu				% Cu d orbital breakdown[c]					%Cys		% Gln		%His	
			Cu[a]	*s*[b]	*p*[b]	*d*[b]	d_{z^2}	d_{xz}	d_{yz}	$d_{x^2-y^2}$	d_{xy}	S	Cys[d]	O	Gln[d]	N[e]	His[d]
50 a	Cu $d_{x^2-y^2}$	−2.99	57	*0*	*2*	*53*	1.2	0.6	0.4	49.4	1.4	30	2	0	0	7	2
49 a	Cu d_{xy}	−3.46	69	*4*	*6*	*57*	16.7	2.3	0.1	3.4	34.5	19	1	2	1	4	4
48 a	Cu d_{z^2}	−3.94	85	*0*	*2*	*81*	56	6.6	0.2	0.1	18.1	1	0.	4	1	5	3
47 a	Cu d_{xz-yz} [f]	−4.08	77	*0*	*1*	*74*	0.2	0.3	72.1	0.5	0.8	5	1	1	0	6	10
46 a	Cu d_{xz+yz} [f]	−4.26	64	*0*	*1*	*61*	0.3	53.2	0.2	0.2	7.1	5	1	0	0	6	23
45 a	His π_1	−4.33	27	*0*	*2*	*22*	1.5	15.9	0.2	4.3	0.1	16	1	0	0	10	45
44 a	Cys π	−4.63	43	*0*	*3*	*37*	2.7	12.4	0.1	20.7	1.1	25	2	0	0	5	25
43 a	His π_1	−4.79	27	*0*	*0*	*25*	1.5	0.1	16.1	6.9	0.4	6	0	1	0	7	58
42 a	Cys pseudo-σ	−5.70	37	*1*	*5*	*28*	4.7	0.2	0.1	0.7	22.2	52	7	1	0	2	1
41 a	Gln O*py*	−6.18	8	*0*	*0*	*6*	5.4	0.0	0.5	0.1	0.0	0	0	54	22	6	8
40 a	His π_2	−6.42	7	*0*	*0*	*5*	0.2	0.9	0.6	0.7	2.5	1	0	2	0	47	42
39 a	His π_2	−6.70	9	*0*	*0*	*7*	0.5	0.0	5.5	0.1	0.9	0	0	16	15	32	29
38 a	Gln O*px*	−6.75	8	*0*	*2*	*4*	2.3	0.4	1.1	0.1	0.1	0	0	39	35	9	6
37 a	Cys σ	−7.49	20	*1*	*6*	*11*	0.4	2.3	1.8	0.0	6.5	49	29	0	0	2	0

[a] Total charge on the copper ion. [b] *l* quantum breakdown for the copper ion. [c] Specific d orbital contributions to the total Cu d charge. [d] Total charge for all atoms of the ligand except the S, O, or N coordinated to Cu. [e] Total charge for the coordinating N atoms. [f] These labels are only strictly valid for C_s symmetry; in the lower symmetry used here, variable amounts of mixing between these orbitals can occur.

spectra of stellacyanin. A single band (2) is required to fit the ∼450 nm absorption intensity, which is labeled band 2 (rather than 1, vide infra) due to its negative CD and MCD sign. Two transitions (3−4) contribute to the ∼600 nm absorption transition envelope. Two transitions of roughly equal intensity (5−6) and a third weaker band (7) at lower energy contribute to the ∼800 nm absorption envelope. A final low energy band (8) is required by the MCD spectrum. No spectral features can be attributed to a transition corresponding to band 1 in plastocyanin, which would exhibit a negative MCD and positive CD sign in the high-energy region of the spectrum.

B. SCF-Xα-SW Calculations. The SCF-Xα-SW calculated ground-state energies and wave functions for the highest occupied valence orbitals obtained with the C_1(gln)(his) approximation of the stellacyanin active site are presented in Table 4. The SCF-Xα-SW calculated half-occupied $d_{x^2-y^2}$ based HOMO (level 50 a, Table 4) in stellacyanin is highly covalent (53% Cu d character), with the predominant Cu−ligand interaction involving 30% S(Cys), and minor contributions from the N(His) atoms (∼7% total). Contours for the half-filled HOMO of stellacyanin are plotted perpendicular and parallel to the O(Gln)-Cu−S(Cys) plane (Figure 5). In stellacyanins the dominant π S(Cys)−Cu antibonding interaction that is found for the HOMO of the classic blue copper plastocyanin[11,15] is clearly evident perpendicular to this plane in Figure 5A. Only minor contributions from S(Cys)−Cu and O(Gln)−Cu σ antibonding interactions can be seen parallel to this plane in Figure 5B. The stellacyanin HOMO (level 50 a) contains no contribution from the axial ligand (i.e., glutamine-based orbitals).

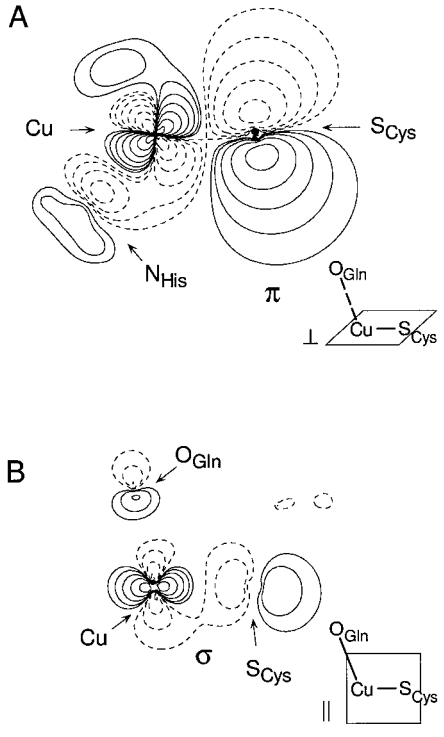

Figure 5. Contours of the highest energy, half-occupied orbital (level 50 a in Table 4) for stellacyanin plotted (A) perpendicular and (B) parallel to the S(Cys)−Cu−O(Gln) plane. Contour lines are drawn at ±0.64, ±0.32, ±0.16, ±0.08, ±0.04, ±0.02, and ±0.01 $(e/bohr^3)^{1/2}$.

The two glutamine-based levels (41 a and 38 a in Table 4), which replace the methionine Met a_1 and b_1 levels, are labeled to indicate the specific O(Gln) p orbital which contributes to the wave function. As the Gln makes no contribution to the half-occupied HOMO, net Cu-Gln bonding is reflected in the amount of Cu 4s and 4p character mixed into the ligand based orbitals. The principal Gln-Cu bonding interaction is found to involve Gln Op*x* (level 38 a) which contains 2−3% Cu 4p (Table 4) (Gln Op*y*, level 41 a, contains <1% Cu 4s and 4p).[42] The Gln Op*x* orbital (level 38 a, Table 4), is composed mainly of the O(Gln) p orbital oriented perpendicular to the amide plane and is depicted in the contour diagram plotted in the O(Gln)−Cu−S(Cys) plane (Figure 1S). The σ Gln−Cu bonding interaction is easily identified by the electron density along the Cu−O(Gln) bond. The orientation of this interaction is approximately that of the Met b_1 orbital in cucumber basic protein. As above, the 1.2% d_{z^2} character mixed into the stellacyanin HOMO (Table 4) is sufficient[34] to generate the observed rhombic EPR splitting.[22]

C. Ligand Field Transitions and Site Geometry. In the low-energy region of the spectra for stellacyanin (<16 000 cm^{-1}), four transitions (bands 5−8) are exhibit large $|C_0/D_0|$ ratios (∼0.1) (Table 3) and are therefore assigned as ligand field transitions (vide supra).[35] These d → d bands for stellacyanin, which exhibit qualitatively similar the CD and MCD spectral features and signs to plastocyanin (Figure 4 and Table 3),[11] can be assigned analogously to those in plastocyanin (Table 3).

Three of the d → d transition energies in the stellacyanin spectra (bands 5−7) shift to much lower energy (1000−2000 cm^{-1}) than their counterparts in plastocyanin.[43] The direction of this shift is in contrast to the shift of the d → d transitions in cucumber basic protein to higher energy (vide supra) and indicates that the type 1 center in stellacyanin experiences a decreased ligand field compared to plastocyanin. Such a decreased ligand field would result from a *tetrahedral* distortion relative to the structure of plastocyanin and not from a tetragonal geometric distortion as in cucumber basic protein and nitrite reductase.[15] The weaker ligand field of stellacyanin relative to plastocyanin, reflected by the 1000−2000 cm^{-1} decrease in d → d energies, results in an increase of g_z in stellacyanin (2.287)[22] relative to that of plastocyanin (2.226).[36]

Changes in the intensity of bands 5 and 6 relative to plastocyanin may reflect changes in ligand−metal bonding in the site. Band 5 intensity increases by a minor amount, but the major change in this region of the spectrum involves band 6 which decreases significantly in intensity (Table 3). The magnitude of the decrease in band 6 (−845 M^{-1} cm^{-1}) is greater than the increase in band 5 (190 M^{-1} cm^{-1}) suggests that rather than a change in Cys π/pseudo-σ character mixing in the HOMO the net S(Cys) covalency has decreased. In particular, the greater energy separation of band 6 and band 4 (the S(Cys) π → Cu $3d_{x^2-y^2}$ charge-transfer transition from which the intensity of band 6 derives, vide supra) in stellacyanin (5600 cm^{-1}) relative to plastocyanin (3900 cm^{-1}) implies that the degree of configuration interaction between the orbitals should be lessened. The SCF-Xα-SW calculations on stellacyanin (Table 4) are consistent with the observed ligand field intensities. Following the analysis presented above, the Cys π orbital (level 44 a) contains 12.4% d_{xz} character and the Cys pseudo-σ orbital (level 42 a) contains very little d_{yz} character (0.1%). Thus, band 6 would be expected to be less intense than its counterpart in cucumber basic protein (16.2% d_{xz} in its Cys π level), and band 5 should not exhibit much increased intensity.

D. Charge-Transfer Transitions and Bonding. Bands 2, 3, and 4 (Figure 4), at higher energy than the ligand field transitions, exhibit smaller C_0/D_0 ratios (∼0.01) which allows for their assignment as charge-transfer transitions (Table 3). Bands 4 and 3 can be assigned in parallel with those in plastocyanin on the basis of energy considerations and correlation of the CD and MCD signs (vide supra).[11] Band 4 in stellacyanin is assigned as the S(Cys) π → Cu $3d_{x^2-y^2}$ charge-transfer transition. Band 3 is assigned as the S(Cys) pseudo-σ → Cu $3d_{x^2-y^2}$ transition. Unlike cucumber basic protein, band 3 in stellacyanin does not shift significantly in energy and it remains within the ∼600 nm envelope as in plastocyanin.[11,15] Bands 2 and 3 in stellacyanin have similar absorption intensities. Compared to the intensities in plastocyanin, in stellacyanin the S(Cys) π → Cu $3d_{x^2-y^2}$ transition (band 4) is reduced while the pseudo-σ → $3d_{x^2-y^2}$ transition (band 3) slightly increased. The limited intensity gain for band 3 and the intensity loss for band 4 indicate that only a minor decrease in π overlap and a slight increase in pseudo-σ S(Cys)−Cu overlap occurs in the stellacyanin HOMO, relative to that of plastocyanin.

The contour plot of the stellacyanin HOMO (Figure 5) reveals that the $d_{x^2-y^2}$ orbital has a π S(Cys)−Cu interaction which is not rotated significantly compared to that of plastocyanin (Figure 5A).[11,15] The relatively minor Cys pseudo-σ character in the HOMO is indicated by the lack of electron density found along the Cu−S(Cys) bond (Figure 5B). The predominantly Cys π interaction with Cu $d_{x^2-y^2}$ is also reflected in the degree to which the specific ligand bonding orbitals mix with the HOMO. Examining the amount of Cu $d_{x^2-y^2}$ character present in the bonding ligand-derived orbitals indicates that the Cys π (level 44 a) contains nearly the same amount of Cu $d_{x^2-y^2}$ character as in plastocyanin (20.7% in STC vs 23.9% in PLC[15]) and there is only a small increase in the amount of Cu $d_{x^2-y^2}$ in the pseudo-σ level (42 a) (0.7% in STC vs 0.0% in PLC[15]). This is in contrast to cucumber basic protein (Table 2), where these value are 12.4% (Cys π) and 2.8% (Cys pseudo-σ), respectively.

The total oscillator strength for the cysteine-based charge-transfer transitions is smaller in stellacyanin (0.0513) than in plastocyanin[15] (0.0544). This indicates that while only minor changes occur in the σ/π overlap involving the S(Cys), the total S(Cys) contribution to the HOMO is less in stellacyanin relative to that in plastocyanin. This result is supported by the reduced S(Cys) covalency in the calculated HOMO (level 50 a, Table 4) (30% in STC vs 35% in PLC[15]). Additionally, the presence of a longer, weaker Cu−S(Cys) bond in stellacyanin relative to plastocyanin is supported by studies which indicate that the HOMO S covalency is 24% vs 38% in plastocyanin,[44] Cu−S(Cys) is longer by ∼0.1 Å,[14] and ν(Cu−S(Cys)) is reduced by ∼40 cm^{-1}.[45]

The single transition found to higher energy than the cysteine-based charge-transfer transitions in stellacyanin (band 2 in Figure 4) is assigned, in parallel with band 2 in plastocyanin, as a His π_1 → Cu $3d_{x^2-y^2}$ charge-transfer transition based on its energy and negative CD sign (band 1 would exhibit a positive CD signal). The absence of band 1, which is typified by a weak negative MCD feature and a prominent positive CD band, in stellacyanin is consistent with the assignment of band 1 as a

(42) Orbital 38 a also contains 4% Cu d_{z^2} mixing; however, the d_{z^2} level (48 a) is fully occupied and does not make a net contribution to bonding.

(43) The remaining ligand field transition (band 8) is found at higher energy than that of plastocyanin but ∼200 cm^{-1} to lower energy relative to azurin (vide infra).

(44) Shadle, S. E., Ph.D. Dissertation, 1994, Stanford University.

(45) Blair, D. F.; Campbell, G. W.; Schoonover, J. R.; Chan, S. I.; Gray, H. B.; Malmstrom, B. G.; Pecht, I.; Swanson, B. I.; Woodruff, W. H.; Cho, W. K.; English, A. M.; Fry, H. A.; Lum, V.; Norton, K. A. *J. Am. Chem. Soc.* **1985**, *107*, 5755−5766.

Met → Cu $3d_{x^2-y^2}$ charge-transfer band in Met containing blue copper sites, such as plastocyanin, cucumber basic protein, and nitrite reductase.

While transitions from Gln Op*y* and Gln Op*x* to the HOMO could occur between 25 000 and 30 000 cm^{-1}, no bands to higher energy than band 2 are observed in the stellacyanin spectra. The SCF-Xα-SW calculated HOMO wave function for stellacyanin includes virtually no O(Gln) character (level 50 a, Table 4) (also see Figure 5). Further, the highest energy Gln valence orbitals (levels 41 a and 38 a, Table 4) contain virtually no $d_{x^2-y^2}$ character (0.1% in both levels). Therefore, the SCF-Xα-SW calculations on the stellacyanin active site (Table 4) indicate that the Gln → Cu charge-transfer transitions should not exhibit appreciable intensity due to lack of orbital overlap.

In summary, the electronic and geometric structure effects responsible for the perturbed spectroscopic features in stellacyanin relative to the classic site in plastocyanin differ significantly from those for the Met containing, perturbed blue copper sites in cucumber basic protein and nitrite reductase.[15] Despite a longer, weaker Cu−S(Cys) bond consistent with other perturbed blue copper sites, very little HOMO rotation occurs and only a small amount of Cys pseudo-σ and no axial ligand character is present in the HOMO. The most striking difference between stellacyanin and cucumber basic protein and nitrite reductase is the lower energy of the ligand field transitions in stellacyanin which reflects a *tetrahedral* rather than tetragonal geometric distortion relative to plastocyanin.

The Blue Copper Sites in *A. denitrificans* Azurin and M121Q. A. Optical Spectroscopic Properties. Low-temperature absorption and MCD spectra in the region from 5000−30000 cm^{-1} for wild type and M121Q *A. denitrificans* azurin are presented in Figure 6 (thick lines). For comparison, the corresponding spectra of plastocyanin and stellacyanin are superimposed (thin lines) on the wild-type azurin and M121Q spectra.

B. Comparison with Plastocyanin and Stellacyanin. The Abs and MCD spectra of *A. denitrificans* azurin are very similar to those of plastocyanin (Figure 6). The blue copper site in azurin exhibits the strong ∼600 nm/weak ∼450 nm absorption intensity pattern associated with classic sites. Furthermore, the d → d bands 5−7 occur at the same energy as their counterparts in plastocyanin, indicating a similar ligand field. Therefore, the electronic structure description for the classic site in plastocyanin[11,15] is applicable to azurin. The ∼1000 cm^{-1} higher energy of band 8 in azurin compared with plastocyanin is consistent with its assignment as the Cu d_{z^2} → Cu $d_{x^2-y^2}$ transition and demonstrates the variability in this transition among classic sites. Band 8 should be shifted to higher energy by the weaker axial (approximately along *z*) interaction in azurin, which is reflected by azurin's ∼0.3 Å longer Cu−S(Met) bond.[46] The notable difference in blue band energy between these sites has been attributed[3] to the number of hydrogen bonds involving the Cys residue (two in azurin vs one in plastocyanin).

The spectra of M121Q and stellacyanin are nearly superimposable (Figure 6A,B). With the exception of an intensity difference in the blue absorption bands (band 4), all transitions in the M121Q spectra occur at the same energies and exhibit similar intensities and C_0/D_0 ratios as their counterparts in stellacyanin. Thus, the description of the stellacyanin electronic structure developed above applies equally to M121Q.

(46) Baker, E. N. *J. Mol. Biol.* **1988**, *203*, 1071−1095.

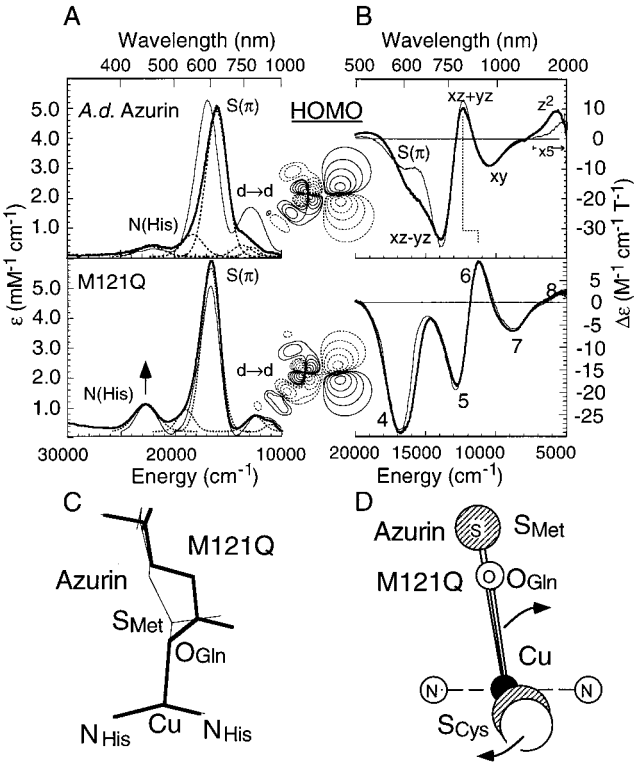

Figure 6. Absorption (A) and low energy MCD (B) spectra of wild type *A. denitrificans* azurin (top), and M121Q azurin (bottom) showing the HOMOs and altered spectral features associated with the increasing *tetrahedral* geometric distortion depicted in panels C and D. Spectra of plastocyanin and stellacyanin (thin lines) are overlaid on the top and bottom panels, respectively. (A) Arrows indicate the direction of the intensity change of the labeled absorption band relative to the classic blue site in *A. denitrificans* azurin. (B) The shift to *lower* energy of the *xz* + *yz* band in the MCD spectra is indicated. The lowest energy band in the MCD has been scaled by a factor of 5. In panel (C) and (D), thick lines (white shading) represent M121Q and thin lines (diagonal shading) represent *A. denitrificans* azurin. In Panel C, Cu−S(Cys) bond extends into the page. Panel D examines the angle between the N_{His}−Cu−N_{His} (extends into the paper) and S_{Cys}−Cu−L_{ax} planes. PLC data and HOMO from ref 15.

Discussion

The electronic structures for the blue (type 1) copper sites in cucumber basic protein, which contains the more prevalent Met Sδ axial ligation,[38] and stellacyanin, which contains Gln Oε axial ligation,[14] have now been defined. In cucumber basic protein, the shift of the d → d transitions to ∼100 cm^{-1} *higher* energy than those in plastocyanin indicates that the site is somewhat more tetragonal than plastocyanin (Figure 7). In stellacyanin, however, the shift of the ligand field transition energies to ∼1000 cm^{-1} *lower* energy than those in plastocyanin (Figure 6) indicates a more tetrahedral geometry. The fact that both tetragonal and tetrahedral distortions of the blue Cu site occur, which result in a redistribution of intensity in the 600/450 nm absorption envelopes and a rhombically split EPR signal,[19−22] illustrates that *either a tetrahedral or tetragonal distortion can result in perturbed blue copper spectral features*. These two classes of perturbed blue copper centers can, however, be differentiated by specific spectroscopic characteristics.

It appears that perturbed blue copper sites with Met axial ligation exhibit geometries along a continuum of the tetragonal distortion from the pseudo-tetrahedral geometry in plastocyanin. In Met-containing perturbed blue Cu sites (i.e., NiR, CBP), the rotation of the $d_{x^2-y^2}$ HOMO relative to plastocyanin causes

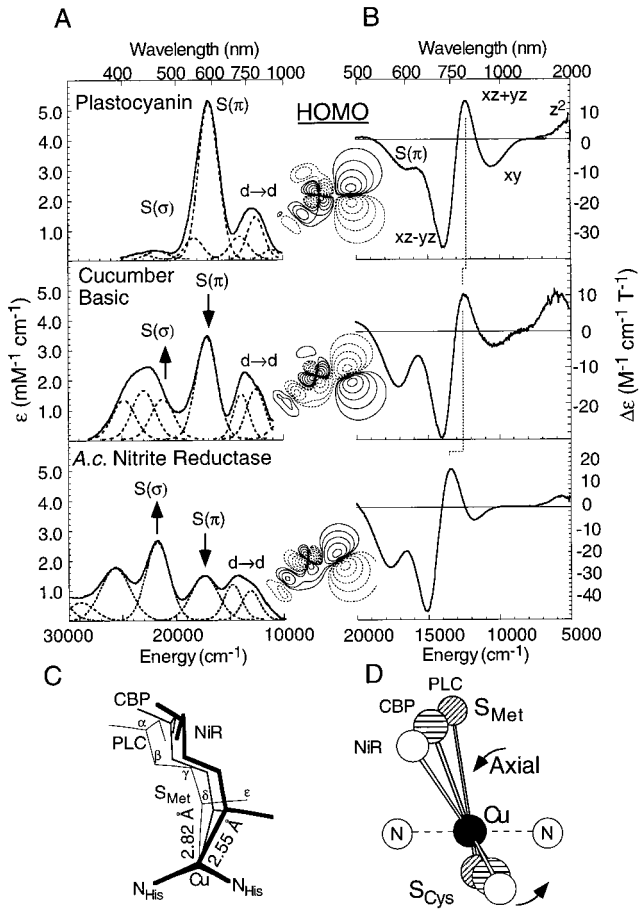

Figure 7. Absorption (A) and low-energy MCD (B) spectra of PLC (top), CBP (middle), and *A. cycloclastes* NiR (bottom) showing the altered spectral features and HOMOs associated with the increasing *tetragonal* geometric distortion depicted in panels C and D. (A) Arrows indicate the direction of the intensity change of the labeled absorption band relative to plastocyanin. (B) Shifts to *higher* energy of the $xz + yz$ band in the MCD spectra are indicated. The lowest energy band in the MCD of PLC, CBP, and NiR has been scaled by a factor of 5. In panel (C) and (D), thick lines (white shading) represent NiR, medium lines (horizontal shading) represent CBP, and thin lines (diagonal shading) represent PLC. In Panel C, Cu−S(Cys) bond extends into the page. Panel D examines the angle between the N_{His}−Cu−N_{His} (extends into the paper) and S_{Cys}−Cu−L_{ax} planes. PLC and NiR data and HOMOs from ref 15.

increased σ and decreased π overlap involving the S(Cys) p and Cu $d_{x^2-y^2}$ orbitals[15] and is a key difference from plastocyanin's classic blue site. This rotation is reflected in the increase of the S(Cys) pseudo-$\sigma \rightarrow$ Cu $3d_{x^2-y^2}$ CT transition intensity (band 3) at the expense of the S(Cys) $\pi \rightarrow$ Cu $3d_{x^2-y^2}$ CT transition (see arrows in Figure 7). This rotation of the $d_{x^2-y^2}$ based HOMO also allows for appreciable mixing of axial S(Met) character into the perturbed HOMO relative to plastocyanin, which also enhances methionine ligand-based charge-transfer intensity (band 1). The degree to which this perturbation occurs increases over the plastocyanin (none, $R_\epsilon \approx 0.1$), cucumber basic protein (moderate, $R_\epsilon \approx 0.6$), nitrite reductase (extreme, $R_\epsilon \approx 1.2$) series is reflected in trends in R_ϵ (Figure 7A) and ligand field transition energies (Figure 7B).

This tetragonal distortion can reflect a Jahn−Teller distorting force that would be present for Cu(II) in a hypothetical intermediate structure (structure 1 in ref 15) with a more tetrahedral geometry resulting from a shorter Cu−S(Met) bond (2.55 Å in NiR[47] vs 2.82 Å in PLC[10]) and a longer Cu−S(Cys) bond (2.17 Å in NiR[47] vs 2.07 Å in PLC[10]) relative to the plastocyanin geometry.[15] This hypothetical intermediate structure would undergo a tetragonal distortion to the nitrite reductase geometry which involves a coupled rotation of the Met ligand toward the NNS(Cys) plane and the Cys ligand within this plane.[15] This distortion approximates the ϵ(u) tetrahedral vibrational mode. The degree to which this distortion occurs can be quantified by measuring the angle between the S(Met)-Cu−S(Cys) and N(His)−Cu−N(His) planes relative to that of plastocyanin. In cucumber basic protein, the 2.61 Å Cu−S(Met) bond[38] corresponds to a $-11.9° \sim\epsilon$(u) distortion. In nitrite reductase, the 2.55 Å Cu−S(Met) bond results in a $-22.8°$ distortion along the $\sim\epsilon$(u) mode. This progressive flattening of the perturbed blue sites with reduction in the axial bond length and the shift in position of the axial residue is illustrated in Figure 7C,D. This distortion also manifests itself in pseudoazurin (2.76 Å Cu−S(Met), $-7.8° \sim\epsilon$(u) mode distortion), which exhibits less perturbed spectral features ($R_\epsilon \approx 0.4$) than cucumber basic protein. It is also present in the azurin mutant[48] M121A/N_3^- which exhibits axial azide binding and shows the $\sim\epsilon$(u) mode distortion to a greater degree (as much as $-35.2°$) than nitrite reductase ($-22.8°$, $R_\epsilon \approx 1.2$).

In contrast to the tetragonally distorted perturbed blue Cu proteins, the electronic structure in stellacyanin does not reveal a significant rotation of the Cu $d_{x^2-y^2}$ based HOMO and no axial ligand charge-transfer transitions are observed even though both classes exhibit perturbed spectral features. Also, relative to plastocyanin, little shift in energy or intensity redistribution of the Cys to Cu charge-transfer transitions occurs in stellacyanin pointing to a unique electronic structure. Instead of the HOMO rotation mechanism, the more limited change in the 600/450 nm absorption intensities associated with stellacyanin appears to be due to increased overlap of the His and S(Cys) pseudo-σ orbitals with the HOMO as a result of the more tetrahedral geometry of this site. The characteristic features of tetrahedrally distorted perturbed blue sites can be summarized as follows: the ligand field transitions shift to lower energy; g_z increases relative to plastocyanin; and little charge-transfer transition absorption intensity attributable to the axial ligand is found at high energy.

The crystal structure of stellacyanin[14] confirms that, as indicated by spectroscopy, the site distorts in the direction of a more tetrahedral structure ($+2°$) relative to plastocyanin. The decreased S(Cys)−Cu stretching frequency,[45] longer Cu−S(Cys) bond length,[14] and lower total Cys oscillator strength in the absorption spectrum of stellacyanin relative to plastocyanin all imply a weaker Cu−S(Cys) interaction resulting from a stronger axial ligand in stellacyanin relative to plastocyanin. According to the argument applied to the tetragonally distorted blue Cu centers,[15] such a situation should induce a Jahn−Teller distortion along the $\sim\epsilon$(u) mode. Two possibilities exist to explain the lack of the expected tetragonal distortion in stellacyanin despite the stronger axial ligand field. It is possible that the axial ligand field strength may be stronger than that in plastocyanin, but has not increased enough to induce a Jahn−Teller distorting force. Alternatively, the protein could resist the Jahn−Teller distortion, enforcing the tetrahedral geometry.

To evaluate the first of these possibilities, the relative strength of the various ligands can be evaluated. The ligand strength will correlate with increased charge donation from the ligand to the Cu ion and increased Cu 4s/4p mixed into the ligand

(47) Adman, E. T.; Godden, J. W.; Turley, S. *J. Biol. Chem.* **1995**, *270*, 27458−27474.
(48) Tsai, L. C.; Bonander, N.; Harata, K.; Karlsson, G.; Vanngard, T.; Langer, V.; Sjolin, L. *Acta Crystallogr., Sect. D: Biol. Crystallogr.* **1996**, *52*, 950−958.

Table 5. Changes in the ADF Calculated Charge Decompositions for the C1(axial)(his) Active Sites of Blue Copper Proteins Relative to Plastocyanin

protein	Δq(cys)[a]	Δq(axial)[b]	Δq(His)[c]	Δ%(4s + 4p)[d]
CBP	*−0.056*	*0.046* [Met]	*0.010*	*4.8%*
NiR	*−0.097*	*0.131* [Met]	*−0.034*	*7.3%*
Stc	*−0.062*	*0.051* [Gln]	*0.011*	*5.0%*

[a] Change in total charge on the thiolate (protein minus plastocyanin). [b] Change in total charge on the axial ligand (protein minus plastocyanin). [c] Change in total charge on both imidazoles (protein minus plastocyanin). [d] Change in total amount of Cu 4s and 4p character summed over all of the axial ligand valence orbitals (protein minus plastocyanin).

orbitals. The changes in the charges on the ligated residues and in the amount of Cu 4s/4p character mixed into the various ligands in cucumber basic protein, nitrite reductase, and stellacyanin relative to those in plastocyanin are summarized in Table 5. ADF density functional calculations on the C_1(axial)(his) approximation to these sites have been employed to avoid the added parameters of sphere radius variation associated with the SCF-Xα-SW method. These results clearly show the increase in the Met ligand strength and decrease in the Cys ligand strength associated with decreasing Cu−S(Met) bond length (and associated longer Cu−S(Cys) bond length) along the tetragonally distorted series. The corresponding values for tetrahedrally distorted stellacyanin indicate that the axial ligand field strength in stellacyanin should be similar to that of tetragonally distorted cucumber basic protein. Because cucumber basic protein is observed to distort −11.9° along the ∼ϵ(u) mode, a measurable tetragonal distortion might be expected for stellacyanin as well.

The expected distorting force along the ∼ϵ(u) mode can also be assessed from the electronic-vibrational linear coupling term,[49] $\delta V/\delta Q_i$ (where V is the potential energy and Q_i is the normal mode of vibration), evaluated over the ground state for stellacyanin. Following ref 49, $\delta V/\delta Q_i$ for the ∼ϵ(u) mode in stellacyanin is calculated to be 0.011 eV/deg, which is significantly greater than that of plastocyanin (0.002 eV/deg) yet only ∼25% of the value of the hypothetical tetrahedral intermediate structure 1 of ref 15 (vide supra) (0.046 eV/deg). This result also supports the assertion that stellacyanin should undergo a modest tetragonal distortion of the magnitude observed in cucumber basic protein.

It is likely then that features of the protein structure in stellacyanin oppose the nonzero distorting force at the blue Cu site and maintain its tetrahedral structure. Stellacyanin, therefore, appears to remain in a rack-induced/entatic condition. However, the protein rack-induced/entatic state in stellacyanin would be somewhat different from that in plastocyanin[8,49] due to the change in ligation. The weak thioether interaction, which the protein structure imposes on the Cu site of plastocyanin, effects increased charge donation from the thiolate which increases the splitting of the d_{xy} and $d_{x^2-y^2}$ orbitals and effectively eliminates the Jahn−Teller distortion in the oxidized site. In stellacyanin, the amide oxygen of the glutamine residue has a somewhat larger axial interaction which weakens the thiolate interaction and reduces the splitting between the d_{xy} and $d_{x^2-y^2}$ orbitals from 10 800 to 8750 cm^{-1} (Table 3). In the absence of additional interactions this should result in a limited Jahn−Teller tetragonal distortion in stellacyanin. This, however, appears to be countered by the nature of the glutamine ligand and/or the protein secondary structure.

While there are a multitude of differences between the structures of plastocyanin, comparison of the structures of wild-type *A. denitrificans* azurin[46] with its M121Q mutant[24] allows for an assessment of the effect of changing only the axial ligand. Relative to wild-type *A. denitrificans* azurin, the axial ligand in M121Q is distorted by +2.9° along the ∼ϵ(u) coordinate (i.e., more tetrahedral, Figure 6C,D), as was anticipated from the spectroscopy (Figure 6A,B) and arguments presented above. Further, the similarity of the spectroscopic features of the M121Q and stellacyanin, which have rather dissimilar secondary structures, suggests that little specialized protein secondary structure is required to create this tetrahedrally distorted blue Cu center. One possible source of rigidity toward ∼ϵ(u) distortion lies in the planar nature of the glutamine ligand, which reduces the number of degrees of freedom available to the side chain compared to the methionine side chain. The nearly identical orientation of the Gln side chain relative to the blue Cu site in the crystal structures of stellacyanin[14] and M121Q[24] suggest that little variation in the orientation of the Gln ligand is possible in comparison to the numerous axial ligand orientations observed in Met containing blue Cu proteins.[3,4,10,38,47,50] Finally, additional interactions, potentially from hydrogen bonding in the site and/or interactions resulting from the carbonyl and NH_2 groups, may also be present and serve to stabilize the tetrahedral geometry observed in stellacyanin.

In summary, variation in axial ligand strength will alter the electronic structure of blue Cu sites. This perturbation associated with a stronger axial bond, concomitant with decreasing S(Cys)−Cu bond strength, will produce a Jahn−Teller distorting force at the blue copper site in the Cu(II) state. For relatively unconstrained axial ligands this results in a tetragonal distortion of the site which increases in magnitude with the strength of the axial ligand. The Jahn−Teller induced tetragonal distortion along the ∼ϵ(u) mode are exemplified along the series plastocyanin < pseudoazurin < cucumber basic protein < nitrite reductase. Since the protein rack-induced/entatic state of the blue Cu site in plastocyanin involves the long axial thioether bond,[49] this tetragonally distorted series of blue Cu sites can be thought of as less entatic.[15] In the case of a more constrained ligand, such as the axial Gln in stellacyanin, the stronger axial interaction results in a more tetrahedral site that is somewhat destabilized by a nonzero Jahn−Teller distorting force in the oxidized state.

Acknowledgment. The authors thank Dr. Michael Lowery for assistance in the preparation of stellacyanin; Prof. Susan Shadle for helpful discussions regarding covalency in these sites; Prof. Andrew Thomson for collection of preliminary stellacyanin MCD data; and Dr. John Hart, Prof. Hans Freeman and Prof. Albrect Messerschmidt for structural information on stellacyanin, cucumber basic protein, and M121Q, respectively. This research was supported by NSF CHE-9528250 (E.I.S.) and NIH GM-28222 (J.S.V.). This work was further supported by the SON and NWO (G.W.C.) as well as a postdoctoral fellowship from the Alexander von Humboldt Foundation (A.M.N.). The computing facilities of the Stanford Department of Chemistry are supported, in part, by a grant from NSF (CHE-9408185).

Supporting Information Available: Tables of Cartesian coordinates and input parameters for SCF-Xα-SW calculations for cucumber basic protein and stellacyanin and a figure of Cu−O(Gln) interaction (3 pages, print/PDF). See any current masthead page for ordering information and Web access instructions.

JA980606B

(49) Guckert, J. A.; Lowery, M. D.; Solomon, E. I. *J. Am. Chem. Soc.* **1995**, *117*, 2817−2844.

(50) Libeu, C. A. P.; Kukimoto, M.; Nishiyama, M.; Horinouchi, S.; Adman, E. T. *Biochemistry* **1997**, *36*, 13160−13179.

(51) Thomson, A. J. Personal communication.